### Title

Accelerated Brain Aging and Cerebral Blood Flow Reduction in Persons With Human Immunodeficiency Virus




### Journal

Clinical Infectious Diseases, 73(10)

### ISSN

1058-4838



### Authors

Petersen, Kalen J
Metcalf, Nicholas
Cooley, Sarah
et al.



### Publication Date

2021-11-16

### DOI

10.1093/cid/ciab169

Peer reviewed

*Clinical Infectious Diseases*

MAJOR ARTICLE

# Accelerated Brain Aging and Cerebral Blood Flow Reduction in Persons With Human Immunodeficiency Virus

**Kalen J. Petersen,[1] Nicholas Metcalf,[1] Sarah Cooley,[1] Dimitre Tomov,[1] Florin Vaida,[2] Robert Paul,[3] and Beau M. Ances[1]**

[1]Department of Neurology, Washington University School of Medicine, St Louis, Missouri, USA; [2]Department of Family and Preventive Medicine, University of California, San Diego, California, USA; and [3]Department of Psychology, University of Missouri, St Louis, Missouri, USA

***Background.*** Persons with human immunodeficiency virus (PWH) are characterized by altered brain structure and function. As they attain normal lifespans, it has become crucial to understand potential interactions between human immunodeficiency virus (HIV) and aging. However, it remains unclear how brain aging varies with viral load (VL).

***Methods.*** In this study, we compare magnetic resonance imaging (MRI) biomarkers among PWH with undetectable VL (UVL; ≤50 genomic copies/mL; n = 230), PWH with detectable VL (DVL; >50 copies/mL; n = 93), and HIV-uninfected ($HIV^-$) controls (n = 206). To quantify gray matter cerebral blood flow (CBF), we utilized arterial spin labeling. To measure structural aging, we used a publicly available deep learning algorithm to estimate brain age from T1-weighted MRI. Cognitive performance was measured using a neuropsychological battery covering 5 domains.

***Results.*** Associations between age and CBF varied with VL. Older PWH with DVL had reduced CBF vs PWH with UVL ($P = .02$). Structurally predicted brain aging was accelerated in PWH vs $HIV^-$ controls regardless of VL ($P < .001$). Overall, PWH had impaired learning, executive function, psychomotor speed, and language compared to $HIV^-$ controls. Structural brain aging was associated with reduced psychomotor speed ($P < .001$).

***Conclusions.*** Brain aging in HIV is multifaceted. CBF depends on age and current VL and is improved by medication adherence. By contrast, structural aging is an indicator of cognitive function and reflects serostatus rather than current VL.

**Keywords.** HIV, aging; cerebral blood flow; brain-predicted age; arterial spin labeling.

The oldest people with human immunodeficiency virus (PWH) in North America have entered their ninth decade, and large, well-characterized clinical cohorts are needed to better understand aging in this population. Human immunodeficiency virus (HIV) may accelerate or accentuate aging by increasing cellular abnormalities or conferring additional risk for comorbidities [1, 2]. The brain is of particular interest, as the central nervous system serves as a potential reservoir even in well-managed PWH. Continued inflammation can lead to neurodegeneration [3] as measured by cortical and subcortical atrophy [4] and white matter degradation [5, 6].

Brain aging may underlie HIV-associated neurocognitive disorders (HAND), which range in severity from asymptomatic impairment to mild neurocognitive deficits to dementia. HAND affects approximately 30% of PWH [7] and contributes to diminished quality of life [8], especially in the older population [9]. Aging is a major risk factor for HAND, compounding cognitive decline associated with normal aging [10].

Neuropsychological improvement and preserved quality of life are possible with combination antiretroviral therapy (cART), suggesting that HIV suppression can modify brain aging [11, 12]. However, previous neuroimaging studies have often treated PWH as a unitary group [13]. Given the ameliorating effects of suppression, it is crucial to quantify how brain aging differs between PWH with variable viral load (VL).

The effects of HIV-related pathology can be assessed with brain-predicted age. In this technique, machine-learning models are trained to estimate chronological age from imaging data, such as T1-weighted magnetic resonance imaging (MRI). Models trained on healthy brains can then be applied to disease states, typically resulting in predicted ages exceeding chronological ages [14, 15]. The difference between these values, brain age gap (BAG), serves as a biomarker of disease-linked structural changes [16].

However, the effects of HIV cannot be understood through structural imaging alone; a more complete picture also requires measurement of functional status to complement anatomical insights from brain-predicted age. A key functional variable is cerebral blood flow (CBF), which governs the rate of oxygen and nutrient delivery to brain parenchyma. CBF is diminished

Received 17 November 2020; editorial decision 14 February 2021; published online 23 February 2021.

Correspondence: K. J. Petersen, Washington University in St Louis, 600 S Euclid Ave, Box 8111, St Louis, MO 63130 (kalen@wustl.edu).

**Clinical Infectious Diseases® 2021;73(10):1813–21**



DOI: 10.1093/cid/ciab169

by HIV [13, 17] as is cerebrovascular reactivity, indicating uncoupling of neural activity from normal vascular responses [18]. Therefore, we applied structural and perfusion neuroimaging to model brain health across the lifespan in a large group of PWH and HIV-uninfected (HIV$^-$) controls. Our goals were to determine how brain aging differs in PWH with detectable viral load (DVL) and undetectable viral load (UVL) compared to normal aging, and whether these phenotypes are associated with cognitive impairment.

## METHODS

### Participants

PWH aged 18 years or older were recruited from the Washington University in St Louis Infectious Diseases Clinic between 2008 and 2017. HIV$^-$ controls were recruited from the St Louis community or research participant registry. Participants provided written informed consent; all studies were approved by the institutional review board.

Exclusion criteria were confounding neurological disorders (eg, epilepsy, stroke), major psychiatric disorders (eg, schizophrenia, bipolar disorder, obsessive-compulsive disorder), Beck Depression Inventory II total score >29, traumatic brain injury with unconsciousness >30 minutes, current or past opportunistic central nervous system infection, or current substance use disorder per the *Diagnostic and Statistical Manual of Mental Disorders, Fifth Edition* (except cannabis). A urinalysis drug screen was administered; participants testing positive for controlled substances other than cannabis were asked to reschedule.

HIV status and VL were assessed with reverse-transcription polymerase chain reaction from blood samples taken during participation. Seronegative status was confirmed for controls. Current CD4 and CD8 cell levels were measured for PWH, and nadir CD4 counts were identified from laboratory or medical records or by participant recall.

PWH were subdivided into 2 categories: those with DVL (RNA loads >50 copies/mL) or UVL (≤50 copies/mL). A subset of participants returned for follow-up imaging and cognitive testing at 1–3 additional time points. Cross-sectional and longitudinal measures were not analyzed separately, but combined using mixed-effects modeling (see "Statistics and Hypothesis Testing," below). Table 1 provides sample sizes for the cross-sectional and longitudinal components of these models.

### Neuroimaging

MRI was performed at 3.0 Tesla on a Tim Trio scanner (Siemens, Erlangen, Germany), and included T1-weighted imaging and pseudo-continuous arterial spin labeling (pCASL). T1-weighted magnetization-prepared rapid gradient echo (T1-MPRAGE) was acquired with a repetition time (TR) of 2400 ms and an echo time (TE) of 3.2 ms at 1-mm isotropic spatial resolution (matrix size = 256 × 256 × 176). pCASL (TR/TE = 3500/9.0 ms) was acquired with label duration = 1500 ms,

**Table 1. Baseline Demographic and Clinical Data**

| Characteristic | HIV-Negative Controls (n = 206) | PWH With UVL (n = 230) | PWH With DVL (n = 93) | *P* Value |
|---|---|---|---|---|
| No. of follow-up visits | 41 | 184 | 26 | |
| Age, y | 36.4 ± 17.1 | 45.9 ± 15.0 | 37.1 ± 16.0 | <.001*** |
| Sex, female, No. (%) | 104 (50) | 56 (24) | 17 (18) | <.001*** |
| Race, African American | 117 (57) | 146 (63) | 72 (77) | .005** |
| Education, y | 13.6 ± 2.4 | 13.3 ± 2.7 | 13.0 ± 1.8 | .09 |
| HIV duration, mo | … | 151.6 ± 106.5 | 76.0 ± 93.6 | <.001*** |
| Current medication duration, mo | … | 50.4 ± 52.2 | 32.5 ± 39.6 | .08 |
| Viral load, copies/mL, $\log_{10}$ | … | 1.3 ± 0.1 | 3.6 ± 1.2 | <.001*** |
| Most recent CD4 count, cells/μL | … | 603.0 ± 287.9 | 390.3 ± 292.7 | <.001*** |
| Nadir CD4 count, cells/μL | … | 213.2 ± 182.7 | 261.4 ± 205.2 | .07 |
| CD4/CD8 ratio | … | 0.79 ± 0.55 | 0.44 ± 0.35 | .01* |
| Hepatitis C infection, No. (%) | … | 15 (7) | 3 (3) | .43 |
| Other STD, No. (%) | 37 (18) | 65 (28) | 16 (17) | .12 |
| BMI | 26.8 ± 5.6 | 26.8 ± 6.0 | 25.8 ± 6.2 | .34 |
| BP (systolic) | 119 ± 16 | 121 ± 12 | 119 ± 15 | .66 |
| BP (diastolic) | 80 ± 11 | 77 ± 12 | 82 ± 11 | .13 |
| Hypertension[a], No. (%) | … | 47/136 (35) | 9/29 (31) | .71 |
| Diabetes[a], No. (%) | … | 12/136 (9) | 1/29 (3) | .33 |

Data are presented as mean ± standard deviation unless otherwise indicated. *P* values are from analysis of variance or Student *t* tests for continuous variables and $\chi^2$ tests for categorical variables.

Abbreviations: BMI, body mass index; BP, blood pressure; DVL, detectable viral load; HIV, human immunodeficiency virus; PWH, persons with human immunodeficiency virus; STD, sexually transmitted disease; UVL, undetectable viral load.

[a]Data available for 162 participants.

*$p$<.05.

**$p$<.01.

***$p$<.001.

postlabeling delay = 1200 ms, flip angle = 90°, spatial resolution = 3.4 × 3.4 × 5 mm, matrix size = 64 × 64 × 22, and 2-dimensional echo-planar imaging readout. Two pCASL runs were obtained per session. Participants were instructed to remain awake and fixate on a crosshair, and monitored for wakefulness.

#### Image Preprocessing and CBF Quantification

Image preprocessing was performed using the FMRIB Software Library (Oxford, United Kingdom). T1-weighted images were brain-extracted and registered to the Montreal Neurological Institute (MNI152) 1-mm brain. pCASL $M_0$ images were affine-registered to T1-weighted images. pCASL volumes were motion-corrected; frame pairs with >0.5-mm displacement between label and control were censored. pCASL images were registered to MNI space and downsampled to 3-mm resolution.

CBF was calculated by pairwise subtraction of spin-tagged and untagged images and application of the standard single-compartment model, following recommended clinical guidelines [19]. Voxels with nonphysiological CBF (<0 or >120 mL/100 g/minute) were excluded. CBF was averaged between runs and quantified across whole-brain gray matter, and in 9 prespecified regions of interest defined using FreeSurfer (Martinos Center, Boston, Massachusetts): frontal cortex, orbitofrontal cortex, sensorimotor cortex, parietal cortex, temporal cortex, occipital cortex, basal ganglia, thalamus, and insula/amygdala.

#### Structural Brain Aging

Brain age was estimated from T1-weighted images using a publicly available deep learning algorithm [20] consisting of a 2D convolutional neural net implemented in Keras. DeepBrainNet was trained on a large dataset including multiple scanners and sites (n = 11 729 participants). Training and validation datasets consisted of healthy individuals across a broad age range. The trained network identified participant age with a mean absolute error of 4.1 years in the original validation cohort.

DeepBrainNet was applied to T1-weighted images to estimate brain age using pretrained weights. Predicted ages were adjusted so the line of best fit for HIV$^-$ controls was linearly shifted to equality (brain age = true age), correcting a well-documented underestimation of brain age in older participants [21]. This transformation did not affect statistical results.

#### Neuropsychological Evaluation

Participants underwent previously described neuropsychological testing to assess 5 domains: learning, delayed recall, executive function, psychomotor speed, and language [22]. Participants were included in cognitive modeling only if they completed at least 10 of 15 total tests. Within each domain, $z$ scores were calculated adjusting for age, sex, race, and education where applicable. A global $z$ score was calculated by averaging across domains.

#### Statistics and Hypothesis Testing

Baseline demographic factors were compared among groups (HIV$^-$ controls, PWH with DVL, and PWH with UVL) using analysis of variance for continuous variables and $\chi^2$ tests for categorical variables. Welch $t$ tests were used for 2-group comparisons applicable only to PWH. Brain aging and cognitive performance were compared with mixed-effects linear models, allowing incorporation of both cross-sectional data for group comparison (fixed effects) and longitudinal measures (random effects).

We predicted that increased VL would be associated with brain aging, measured by decreased CBF and increased BAG. These predictions were tested using R version 4.0.1 (R Foundation, Vienna) with the "nlme" package. The following mixed effects models were used: $(CBF \text{ or BAG}) \sim \beta_1\,(age \times group) + \beta_2\,(sex) + \beta_3\,(race) + U_{participant} + \Psi$, where age × group is an interaction, $U_{participant}$ represents random normal participant effects, and $\Psi$ is the residual distribution model. Two comparisons were made: all PWH vs controls, and PWH with DVL vs UVL.

We also predicted that CBF and structural aging would be associated with cognitive performance. This was tested with the following models: $z - score \sim \beta_1\,(CBF\ or\ BAG) + \beta_2\,(group) + \beta_3\,(age) + U_{participant} + \Psi$. Sex and race were not included in these models as cognitive scores were already adjusted for these factors using normative procedures for each test. As an additional analysis, we tested wither cognitive function was associated with HIV duration: $z - score \sim \beta_1(duration_{HIV}) + \beta_2(group) + \beta_3(age)$. Cognitive $P$ values were corrected for multiple comparisons across 5 cognitive domains by controlling the false discovery rate at 5%. Corrected $P$ values are reported.

## RESULTS

#### Demographics

Five hundred twenty-nine participants met inclusion criteria at baseline: 206 HIV$^-$ controls, 230 PWH with UVL, and 93 PWH with DVL. Two hundred participants returned for follow-up imaging and testing (Supplementary Table 1): 200 second visits (1.9 ± 0.8 years after baseline), 40 third visits (3.3 ± 1.5 years), and 10 fourth visits (5.4 ± 1.8 years). VL status was assigned independently per visit; a participant could be classed as DVL at baseline and UVL at follow-up, or vice versa. Of 780 imaging sessions, 689 included pCASL; the remainder were used for structural aging and cognitive analysis. Demographic and clinical information are presented in Table 1. Age distributions are shown in Supplementary Figure 1.

Participant groups were similar at baseline for education, body mass index, blood pressure, time on current antiretroviral regimen, and prevalence of non-HIV sexually transmitted diseases. Groups differed by age ($P < .001$), sex

($P < .001$), and race ($P = .005$), controlled for in subsequent modeling. Disease duration was longer in PWH with UVL ($P < .001$) due to greater age. CD4 levels ($P < .001$) and CD4/CD8 ratios ($P = .01$) were lower for DVL than UVL subgroups. Mean CD4/CD8 ratios for both HIV groups were <1, indicating elevated risk for adverse events. Neither nadir CD4 count nor hepatitis C rate differed between DVL and UVL subgroups.

#### CBF Is Reduced in Older PWH With DVL

As expected, gray matter CBF was negatively correlated with age ($P < .001$) (see Supplementary Table 2 for effect sizes and confidence intervals). The association between CBF and age was significantly more negative for DVL than UVL with an interaction observed ($P = .02$; Figure 1). CBF-vs-age slope was also more negative in 7 of 9 regions of interest: frontal cortex ($P = .04$), orbitofrontal cortex ($P = .03$), sensorimotor cortex ($P = .04$), occipital cortex ($P = .03$), temporal cortex ($P = .04$), basal ganglia ($P = .03$), and insula/amygdala ($P = .04$ (Supplementary Figure 2). The CBF-vs-age slope was not significantly different between all PWH and HIV$^-$ controls. Figure 2 shows CBF maps by age and group.

#### Structural Aging Is Accelerated in PWH

Structural aging was evaluated by measuring BAG, the discrepancy between brain-predicted and chronological age. DeepBrainNet predicted age with a mean absolute error of 5.2 years for controls, 7.4 years for PWH with UVL, and 7.8 years for PWH with DVL. Structural aging was greater for PWH than HIV$^-$ controls ($P < .001$), but not different between DVL and UVL subgroups (Figure 3).

#### Altered Cognition Is Associated With HIV and DVL

Cognitive function was reduced in PWH vs HIV$^-$ controls in 3 domains: executive function ($P > .001$), psychomotor speed ($P > .001$), and language ($P > .001$). Global cognition was reduced in both PWH subgroups vs HIV$^-$ controls ($P > .001$). Cognition was reduced in DVL vs UVL in 2 domains: psychomotor speed ($P = .003$) and language ($P = .01$). Global cognition was reduced in DVL vs UVL ($P = .003$) (Table 2).

#### Structural Aging Is Associated With Reduced Psychomotor Speed

No association was found between cognitive performance and CBF. A negative relationship was found between BAG and psychomotor $z$ score across participants, independent of group

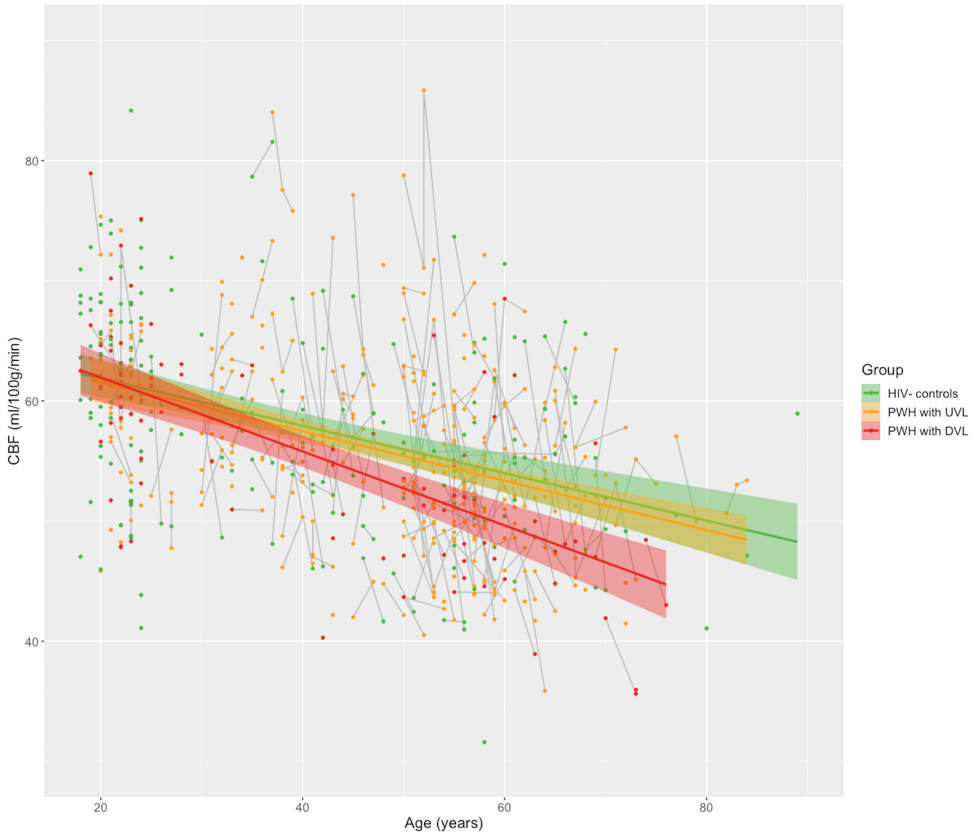


**Figure 1.** Cerebral blood flow is more negatively associated with age in persons with human immunodeficiency virus (HIV) who have detectable viral load (DVL). Gray matter cerebral blood flow (CBF) has a more negative relationship with age in people with DVL (>50 copies/mL; red) than undetectable viral load (UVL) (orange), an age × group interaction ($P = .02$). By contrast, CBF age association was not different between PWH with UVL and HIV-uninfected controls. Repeated measures of the same participant are represented with gray lines.

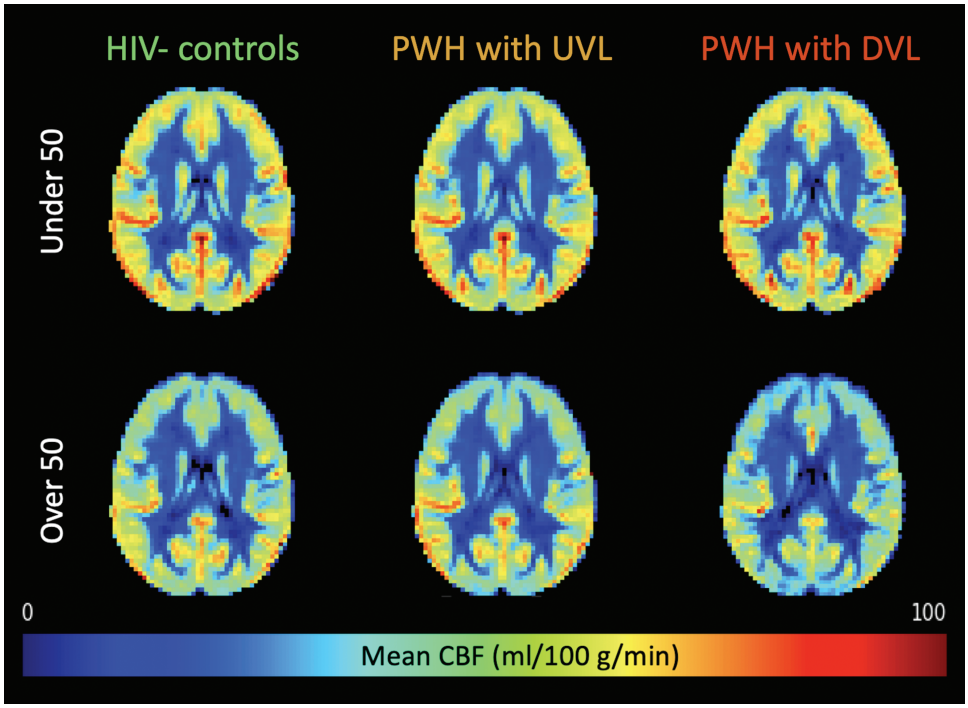


**Figure 2.** Cerebral blood flow depends on age and viral load (VL). Mean cerebral blood flow (CBF) for persons aged >50 or ≤50 years belonging to each study group are represented in standard space. Younger participants showed similar CBF regardless of disease group (top row). Among older participants (bottom row), persons with human immunodeficiency virus with detectable VL (bottom right) had reduced CBF, reflecting an interaction between age and VL. Abbreviations: DVL, detectable viral load; HIV, human immunodeficiency virus; PWH, people with human immunodeficiency virus; UVL, undetectable viral load.

or chronological age ($P < .001$) (Figure 4). Duration of infection was positively associated with learning ($P = .006$), delayed recall ($P = .006$), and total cognition ($P = .006$).

## DISCUSSION

We found evidence of altered brain functional and structural aging in PWH. Older PWH with DVL had reduced gray matter CBF, while those with UVL had CBF comparable to HIV$^-$ controls. In contrast, structural brain aging was accelerated in both HIV subgroups. Cognitive performance varied by serostatus, with impaired executive function, psychomotor speed, and language observed in PWH compared to HIV$^-$ controls. Psychomotor and language function were further impaired in the DVL subgroup. Structural aging was associated with psychomotor slowing across all participants. Overall, these data support a connection between HIV and pathological brain aging.

We identified DVL and age as risk factors for diminished CBF. Previous work has found reduced CBF in PWH [13], although other studies have shown little difference [17] or even increased CBF due to HIV [23]. These discrepancies may relate to relatively small sample sizes or younger participants. Differentiation of PWH into DVL and UVL may be a crucial difference, as previous studies have typically combined these subgroups, who we find to follow distinct trajectories. While the underlying biology is unclear, CBF preservation in those with UVL suggests that cART may maintain or improve brain function. Conversely, older PWH with DVL may be more sensitive to HIV-induced pathologies such as inflammation, endothelial dysfunction, or capillary permeability [24, 25]. CBF reduction might also reflect comorbid cardiovascular disease or coinfections such as hepatitis C [26, 27]. However, we note that body mass index, blood pressure, hypertension, diabetes, and hepatitis C rates were similar between VL subgroups, suggesting that these factors may not explain our observations.

We did not observe associations between CBF and cognitive function. Several prior studies, including one with 100 virologically suppressed PWH, found no differences in CBF between cognitively impaired and unimpaired PWH [28]. An early study found a relationship between CBF and the HIV dementia scale; however, these participants had severe impairments rather than milder forms of HAND that are increasingly common in the cART era [29]. Thus, our results remain consistent with current literature, and support the conclusion that resting CBF is not primarily related to HIV cognitive impairment, but rather a function of current VL.

While reduced CBF was specific to older PWH with DVL, accelerated structural aging was observed even in those with UVL. This may imply that structural aging results from a legacy effect of early tissue damage or is cART resistant. Our data are congruent with previous findings that PWH have reduced gray matter volume [4, 30–32] and diminished white matter


**Figure 3.** Structural aging is accelerated in persons with human immunodeficiency virus (PWH). Brain age was predicted using a deep-learning model on T1-weighted images. *A*, PWH with both detectable (red) and undetectable (orange) viral load showed increasing overestimation of brain age with increasing chronological age, as compared with human immunodeficiency virus (HIV)–negative controls (green) ($P < .001$). Structural aging did not significantly differ between the HIV subgroups. Gray lines represent repeated measures. *B*, Residuals for structurally predicted vs actual age (brain age gap). Abbreviations: DVL, detectable viral load; UVL, undetectable viral load.

integrity [5, 6]. Such degeneration, representing irreversible cell death, may explain why structural aging was independent of current VL.

Structural brain age was predicted using deep learning. This technique can distinguish subtle nonlinear relationships between morphology and neuropathology [14, 15]. Our findings are consistent with previous literature showing that HIV ages the brain [16, 33]. For this analysis we utilized a publicly available brain age estimator, DeepBrainNet, developed to promote reproducible and generalizable age prediction. DeepBrainNet is more accurate at disease classification than widely used databases such as ImageNet [20]. Unlike most age-prediction models, which depend on preprocessing to define discrete training features, DeepBrainNet uses minimally preprocessed volumetric T1 images as input, reducing methodological variability and allowing easier standardization across sites. DeepBrainNet has been successfully used to classify other neurodegenerative diseases including Alzheimer disease and schizophrenia [20].

Deep learning has been previously used to predict age from structural MRI of PWH. Cole et al trained a convolutional neural network on a large normative dataset and achieved high

**Table 2. Cognitive Function in Study Participants**

| | All PWH vs Controls | | PWH With DVL vs PWH With UVL | |
|---|---|---|---|---|
| Domain | Effect (95% CI) | *P* Value | Effect (95% CI) | *P* Value |
| Learning | −0.16 (−.34 to .01) | .07 | −0.21 (−.41 to .00) | .08 |
| Delayed recall | −0.10 (−.29 to .09) | .29 | −0.20 (−.45 to .05) | .13 |
| Executive | −0.38 (−.53 to −.23) | >.001*** | −0.11 (−.28 to .06) | .22 |
| Psychomotor | −0.28 (−.42 to −.14) | >.001*** | −0.24 (−.38 to −.10) | .003** |
| Language | −0.39 (−.54 to −.23) | >.001*** | −0.25 (−.42 to −.08) | .01* |
| Global | −0.31 (−.42 to −.20) | >.001*** | −0.20 (−.32 to −.08) | .003** |

Effect of HIV and detectable viral load on cognitive *z* scores. Tests were normalized for age, sex, race, and years of education. The global *z* score represents the mean across domains. Results from mixed-effects linear models are given, and *P* values are corrected for multiple comparisons across domains.

Abbreviations: CI, confidence interval; DVL, detectable viral load; PWH, persons with human immunodeficiency virus; UVL, undetectable viral load.

*$P < .05$.

**$P < .01$.

***$P < .001$.

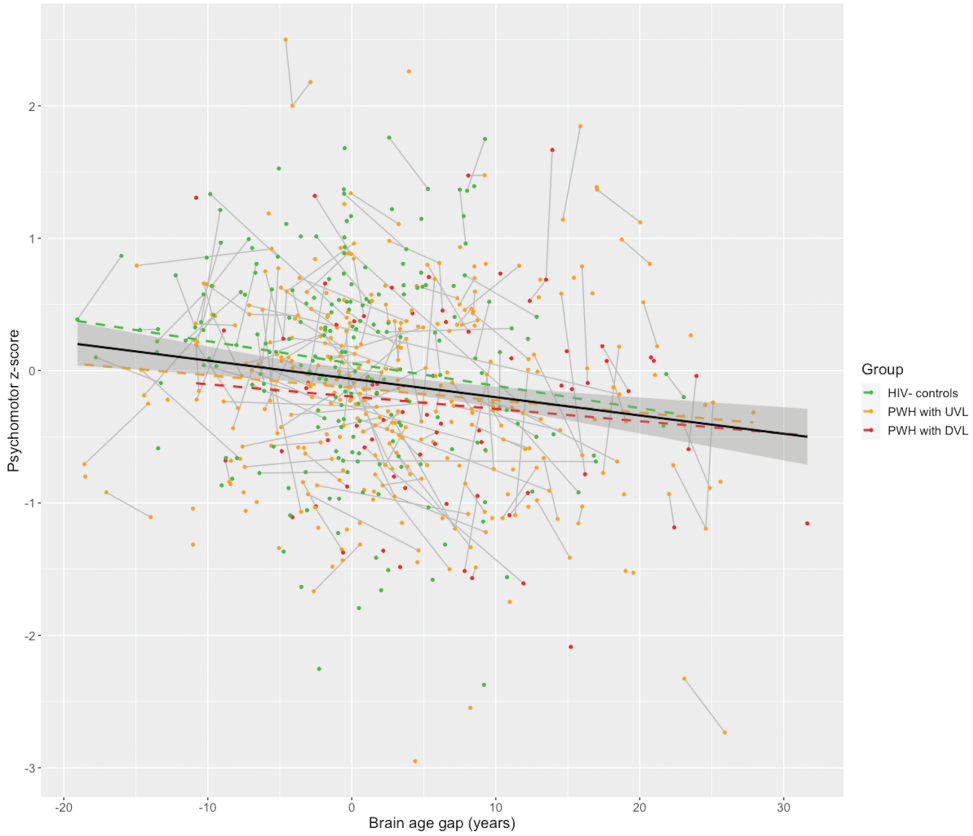


**Figure 4.** Psychomotor function reflects structural aging. Structural brain aging, as measured by the gap between predicted and chronological age (brain age gap), negatively correlates with psychomotor speed ($P < .001$). The black trendline represents the relationship across all participants, controlling for disease group and chronological age. Dashed, colored trendlines show relationships within disease subgroups. Gray connecting lines are repeated measures of the same participant. Abbreviations: DVL, detectable viral load; HIV, human immunodeficiency virus; PWH, people with human immunodeficiency virus; UVL, undetectable viral load.

predictive accuracy in training and testing [34]. They found greater BAG in PWH, but no age interaction, possibly due to the limited number of older PWH who were included. Notably, the brain-age graph by Cole et al does suggest a trend toward different slopes for PWH and HIV$^-$ controls (their Figure 3). The same interaction might be present in both their study and ours, if a larger sample size was used. This may also apply to Kuhn et al [33], who likewise detected greater BAG in PWH using diffusion imaging. No age × group interaction was observed, possibly due to the difficulty of detecting such effects with relatively few older PWH.

In the current analysis, structural aging was associated with cognitive dysfunction. Cognitive impairment in PWH has previously been shown to be associated with reduced cortical thickness [32] and tissue volume loss [30]. We found that diminished psychomotor speed was linked with structural BAG, independent of disease status. Psychomotor function is often diminished in PWH [35] but improves with cART [36]. Our results remain broadly consistent with those of Cole et al, who found correlations between BAG and neuropsychological function.

The absence of correlation between structural BAG and domains other than psychomotor function should not be taken as contradicting existing literature. Abundant evidence connects brain structural changes with cognitive impairment in PWH [29, 37–39]. However, past studies have focused on volumetric changes in specific brain regions, whereas our approach produced a single summary statistic of whole-brain structural aging, promoting simplicity over regional specificity. Future modeling with restricted regional input might reveal cognitive relationships not evident in our current results. Structural age likely reflects widespread and subtle cerebral changes related to HIV neuropathogenesis, beginning with early insults and manifesting as cumulative degeneration in later years, even in virologically well-controlled PWH. Thus, BAG may be thought of as a stable summary measure, in contrast to CBF, which varies over short timescales and is dynamically responsive to VL.

While this study is one of the largest examinations of brain structural and functional changes in PWH to date, it should be considered in the context of several limitations. First, separation of PWLH into VL subgroups relied on recent viral titers, which may reflect transient changes or "blips" in HIV proliferation. Nonetheless, current VL provides a reasonable approximation of disease severity, particularly in a large

population. Moreover, our statistical framework allowed flexible categorization of participants between time points if VL changed. Secondly, nadir CD4 cell counts were self-reported in some cases, though they were verified when possible from electronic medical records. Self-reported values are less reliable, and may explain why HIV groups did not differ in nadir CD4 ($P = .07$). Third, data on hypertension and diabetes were only available for a subset of PWH (n = 162). This subset was similar to the larger PWH group in sex, race, and education, though significantly older ($P < .001$). Within this subset, we found no difference in hypertension or diabetes rates between DVL and UVL. Finally, our disease groups differed in age, sex, and race, though these factors were controlled for in statistical models.

Taken together, our findings suggest that age-related effects in PWH are two-fold. Structural aging consists of physical alterations detectable by conventional MRI, including gray and white matter degeneration independent of VL. In contrast, CBF involves dynamic, VL-responsive changes at the vascular level, which may be mitigated by cART. Although cART itself is linked to neurological side effects [40], our observations suggest that HIV suppression preserves normal perfusion. In both CBF and volumetrics, HIV and aging interact to promote phenotypic changes, steepening the slope of pathology curves. However, these data do not rule out accentuation by comorbidities [2]. Future work with more extended longitudinal follow-up may determine whether neuroimaging measures are causally linked with successful viral suppression, or partly attributable to concurrent risk factors.

## Supplementary Data

Supplementary materials are available at *Clinical Infectious Diseases* online. Consisting of data provided by the authors to benefit the reader, the posted materials are not copyedited and are the sole responsibility of the authors, so questions or comments should be addressed to the corresponding author.

## Notes

***Acknowledgments.*** The authors express their gratitude to all study participants for making this study possible. The authors are grateful to Peter Millar for technical advice and Vishnu Bashyam for assistance with DeepBrainNet.

***Financial support.*** This work was supported by the National Institute of Mental Health (grant number R01MH118031) and the National Institute of Nursing Research (grant numbers R01NR015738, R01NR012907, R01NR012657, and R01NR014449).

***Potential conflicts of interest.*** The authors: No reported conflicts of interest. All authors have submitted the ICMJE Form for Disclosure of Potential Conflicts of Interest.

## References

1. Horvath S, Levine AJ. HIV-1 infection accelerates age according to the epigenetic clock. J Infect Dis **2015**; 212:1563–73.
2. Pathai S, Bajillan H, Landay AL, High KP. Is HIV a model of accelerated or accentuated aging? J Gerontol A Biol Sci Med Sci **2014**; 69:833–42.
3. Valcour V, Sithinamsuwan P, Letendre S, Ances B. Pathogenesis of HIV in the central nervous system. Curr HIV/AIDS Rep **2011**; 8:54–61.
4. Küper M, Rabe K, Esser S, et al. Structural gray and white matter changes in patients with HIV. J Neurol **2011**; 258:1066–75.
5. Seider TR, Gongvatana A, Woods AJ, et al. Age exacerbates HIV-associated white matter abnormalities. J Neurovirol **2016**; 22:201–12.
6. Zhu T, Zhong J, Hu R, et al. Patterns of white matter injury in HIV infection after partial immune reconstitution: a DTI tract-based spatial statistics study. J Neurovirol **2013**; 19:10–23.
7. Sacktor N, Skolasky RL, Seaberg E, et al. Prevalence of HIV-associated neurocognitive disorders in the Multicenter AIDS Cohort Study. Neurology **2016**; 86:334–40.
8. Tozzi V, Balestra P, Murri R, et al. Neurocognitive impairment influences quality of life in HIV-infected patients receiving HAART. Int J STD AIDS **2004**; 15:254–9.
9. Doyle K, Weber E, Atkinson JH, Grant I, Woods SP; HIV Neurobehavioral Research Program (HNRP) Group. Aging, prospective memory, and health-related quality of life in HIV infection. AIDS Behav **2012**; 16:2309–18.
10. Wendelken LA, Valcour V. Impact of HIV and aging on neuropsychological function. J Neurovirol **2012**; 18:256–63.
11. Parsons TD, Braaten AJ, Hall CD, Robertson KR. Better quality of life with neuropsychological improvement on HAART. Health Qual Life Outcomes **2006**; 4:1–7.
12. Zhuang Y, Qiu X, Wang L, et al. Combination antiretroviral therapy improves cognitive performance and functional connectivity in treatment-naïve HIV-infected individuals. J Neurovirol **2017**; 23:704–12.
13. Ances BM, Sisti D, Vaida F, et al; HNRC Group. Resting cerebral blood flow: a potential biomarker of the effects of HIV in the brain. Neurology **2009**; 73:702–8.
14. Gaser C, Franke K, Klöppel S, Koutsouleris N, Sauer H; Alzheimer's Disease Neuroimaging Initiative. BrainAGE in mild cognitive impaired patients: predicting the conversion to Alzheimer's disease. PLoS One **2013**; 8:e67346.
15. Koutsouleris N, Davatzikos C, Borgwardt S, et al. Accelerated brain aging in schizophrenia and beyond: a neuroanatomical marker of psychiatric disorders. Schizophr Bull **2014**; 40:1140–53.
16. Cole JH, Underwood J, Caan MWA, et al. Increased brain-predicted aging in treated HIV disease. Neurology **2017**; 88:1349–57.
17. Towgood KJ, Pitkanen M, Kulasegaram R, et al. Regional cerebral blood flow and FDG uptake in asymptomatic HIV-1 men. Hum Brain Mapp **2013**; 34:2484–93.
18. Callen AL, Dupont SM, Pyne J, et al. The regional pattern of abnormal cerebrovascular reactivity in HIV-infected, virally suppressed women. J Neurovirol **2020**; 26:734–42.
19. Alsop DC, Detre JA, Golay X, et al. Recommended implementation of arterial spin-labeled perfusion MRI for clinical applications: a consensus of the ISMRM perfusion study group and the European consortium for ASL in dementia. Magn Reson Med **2015**; 73:102–16.
20. Bashyam VM, Erus G, Doshi J, et al. MRI signatures of brain age and disease over the lifespan based on a deep brain network and 14 468 individuals worldwide. Brain **2020**; 143:2312–24.
21. Le TT, Kuplicki RT, McKinney BA, Yeh HW, Thompson WK, Paulus MP; Tulsa 1000 Investigators. A nonlinear simulation framework supports adjusting for age when analyzing BrainAGE. Front Aging Neurosci **2018**; 10:317.
22. Paul RH, Cooley SA, Garcia-Egan PM, Ances BM. Cognitive performance and frailty in older HIV-positive adults. J Acquir Immune Defic Syndr **2018**; 79:375–80.
23. Sen S, An H, Menezes P, et al. Increased cortical cerebral blood flow in asymptomatic human immunodeficiency virus-infected subjects. J Stroke Cerebrovasc Dis **2016**; 25:1891–5.
24. Chaganti J, Marripudi K, Staub LP, et al. Imaging correlates of the blood-brain barrier disruption in HIV-associated neurocognitive disorder and therapeutic implications. AIDS **2019**; 33:1843–52.
25. Cysique LA, Brew BJ. Vascular cognitive impairment and HIV-associated neurocognitive disorder: a new paradigm. J Neurovirol **2019**; 25:710–21.
26. Kompella S, Al-Khateeb T, Riaz OA, et al. HIV-associated neurocognitive disorder (HAND): relative risk factors [manuscript published online ahead of print 28 July 2020]. Curr Top Behav Neurosci **2020**. doi:10.1007/7854_2020_131.
27. Rodriguez-Penney AT, Iudicello JE, Riggs PK, et al; HIV Neurobehavioral Research Program HNRP Group. Co-morbidities in persons infected with HIV: increased burden with older age and negative effects on health-related quality of life. AIDS Patient Care STDS **2013**; 27:5–16.
28. Su T, Mutsaerts HJMM, Caan MWA, et al. Cerebral blood flow and cognitive function in HIV-infected men with sustained suppressed viremia on combination antiretroviral therapy. AIDS **2017**; 31:847–56.
29. Chang L, Ernst T, Leonido-Yee M, Speck O. Perfusion MRI detects rCBF abnormalities in early stages of HIV-cognitive motor complex. Neurology **2000**; 54:389–96.
30. Becker JT, Maruca V, Kingsley LA, et al; Multicenter AIDS Cohort Study. Factors affecting brain structure in men with HIV disease in the post-HAART era. Neuroradiology **2012**; 54:113–21.

31. O'Connor EE, Zeffiro TA, Zeffiro TA. Brain structural changes following HIV infection: meta-analysis. AJNR Am J Neuroradiol **2018**; 39:54–62.
32. Sanford R, Fernandez Cruz AL, Scott SC, et al. Regionally specific brain volumetric and cortical thickness changes in HIV-infected patients in the HAART era. J Acquir Immune Defic Syndr **2017**; 74:563–70.
33. Kuhn T, Kaufmann T, Doan NT, et al. An augmented aging process in brain white matter in HIV. Hum Brain Mapp **2018**; 39:2532–40.
34. Cole JH, Poudel RPK, Tsagkrasoulis D, et al. Predicting brain age with deep learning from raw imaging data results in a reliable and heritable biomarker. Neuroimage **2017**; 163:115–24.
35. Manly JJ, Smith C, Crystal HA, et al. Relationship of ethnicity, age, education, and reading level to speed and executive function among HIV+ and HIV- women: the Women's Interagency HIV Study (WIHS) Neurocognitive Substudy. J Clin Exp Neuropsychol **2011**; 33:853–63.
36. Sacktor NC, Lyles RH, Skolasky RL, et al. Combination antiretroviral therapy improves psychomotor speed performance in HIV-seropositive homosexual men. Multicenter AIDS Cohort Study (MACS). Neurology **1999**; 52:1640–7.
37. Bonnet F, Amieva H, Marquant F, et al. Cognitive disorders in HIV-infected patients: are they HIV-related? AIDS **2013**; 27:391–400.
38. Cohen RA, Harezlak J, Schifitto G, et al. Effects of nadir CD4 count and duration of human immunodeficiency virus infection on brain volumes in the highly active antiretroviral therapy era. J Neurovirol **2010**; 15:25–32.
39. Patel SH, Kolson DL, Glosser G, et al. Correlation between percentage of brain parenchymal volume and neurocognitive performance in HIV-infected patients. AJNR Am J Neuroradiol **2002**; 23:543–9.
40. O'Halloran JA, Cooley SA, Strain JF, et al. Altered neuropsychological performance and reduced brain volumetrics in people living with HIV on integrase strand transfer inhibitors. AIDS **2019**; 33:1477–83.